J Toxicol Pathol 2021; 34: 339–343

Case Report

Spontaneous cholangiofibrosis adjacent to a dilated common bile duct with intestinal metaplasia in a Royal College of Surgeons rat

Kiyokazu Ozaki[1]*, Yui Terayama[1], and Tetsuro Matsuura[1]

[1] Laboratory of Pathology, Faculty of Pharmaceutical Sciences, Setsunan University, 45-1 Nagaotoge-cho, Hirakata, Osaka 573-0101, Japan

Abstract: A 130-week-old male Royal College of Surgeons rat kept as a non-treated animal in a long-term animal study presented with a mass in the hepatic portal region that adhered to a dilated common bile duct and the duodenum. Histopathologically, the solitary mass showed expansive growth with no apparent compression and continued to dilate the common bile duct, which had a hyperplastic epithelium with intestinal metaplasia. The mass mainly consisted of small to large dilated and/or tortuous ducts with abundant dense connective tissue and many inflammatory cells. The single-layer lining epithelium of the duct changed from cuboidal to columnar. Immunohistochemically, the lining cells were positive for cytokeratin 7, cytokeratin 19, and OV-6, which are bile duct markers. Based on the pathological characteristics, the rat was diagnosed as spontaneous cholangiofibrosis adjacent to a dilated common bile duct with intestinal metaplasia. (DOI: 10.1293/tox.2021-0032; J Toxicol Pathol 2021; 34: 339–343)

Key words: cholangiofibrosis, rat, liver, bile duct, metaplasia

Cholangiofibrosis, as defined by the International Harmonization of Nomenclature and Diagnostic Criteria (INHAND), is a proliferative and metaplastic biliary reaction with fibrosis extending into the hepatic parenchyma[1]. Various xenobiotics such as dioxins, furans, thioacetamides, and *Fusarium moniliforme* can induce cholangiofibrosis[2–4]. Spontaneous cholangiofibrosis in untreated rats is extremely rare and has only been reported in a case of a Wistar rat and characteristic lesions of a Long-Evans Cinnamon (LEC) rat[5, 6]. However, the LEC rat was a model of Wilson's disease, and cholangiofibrosis was caused by a genetic predisposition to hepatotoxicity[6]. Recently, we encountered a case of cholangiofibrosis in a male Royal College of Surgeons (RCS)/Kyo rat with no genetic predisposition to hepatotoxicity. This report describes the histological characteristics of cholangiofibrosis in this RCS rat.

RCS rats are an inbred strain and are well known for their predisposition to inherit retinal degeneration; they have no genetic predisposition to hepatotoxicity[7, 8]. RCS/Kyo rats were maintained at the National BioResource Project-Rat (NBRP-Rat) facility of Kyoto University (Japan). They were maintained as an inbred strain by full-sibling mating. Among them was a 130-week-old RCS male rat that was reserved as a non-treated animal in a long-term study and fed a standard diet (Charles River Formula 1; Oriental Yeast Co., Ltd., Tokyo, Japan) with chlorinated water *ad libitum*. It was kept in an animal room maintained at a temperature of 24 ± 2 °C with a relative humidity of 60 ± 20%, a 12 h light/dark cycle, and ventilation at least 12 times/h. Apart from coarse hair, no clinical signs were apparent until the scheduled sacrifice at 130 weeks of age. The rat was deeply anesthetized using ketamine (40 mg/kg, intramuscular [IM]; Ketalar, Sankyo, Tokyo, Japan) and xylazine (2.0 mg/kg, IM; Seractal, Bayer, Tokyo, Japan) and euthanized by exsanguination. The study was approved by the Committee for Animal Experiments of Setsunan University.

A gross mass of 20 × 10 × 10 mm was observed in the hepatic portal region. The mass adhered to a dilated common bile duct and the duodenum. The mass was soft, and the cut surface was composed of multiple small to large cysts (Fig. 1). Specimens were fixed in 10% neutral phosphorylated formalin (pH 7.4), dehydrated in a graded series of ethanol, and embedded in paraffin. Sections (4 µm) were subsequently stained with hematoxylin and eosin, Alcian blue (AB) stain, and periodic acid-Schiff reaction (PAS). Immunohistochemical staining using a labeled polymer method was performed using N-Histofine MAX PO rat (M or R) (Nichirei, Tokyo, Japan). The following primary antibodies were used: anti-Ki-67 (1:400, rabbit monoclonal antibody; Abcam, Cambridge, UK), anti-oval cell marker (OV-6) (1:100, mouse monoclonal antibody; Santa Cruz Biotechnology, CA, USA), anti-cytokeratin 19 (1:50, rabbit polyclonal antibody; Abcam), and anti-cytokeratin 7 (1:20, mouse monoclonal antibody; DAKO, Glostrup, Denmark)[9].

Received: 26 May 2021, Accepted: 28 June 2021
Published online in J-STAGE: 17 July 2021
*Corresponding author: K Ozaki
(e-mail: ozaki@pharm.setsunan.ac.jp)

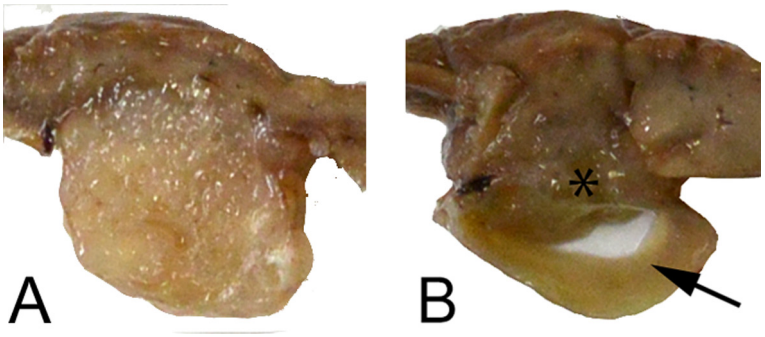

Fig. 1. Gross appearance of 20 × 10 × 10 mm mass in the hepatic portal region. **A**: The cut surface was composed of multiple cysts of various sizes. **B**: Image of mass (asterisk) adhered to the dilated common bile duct (arrow).

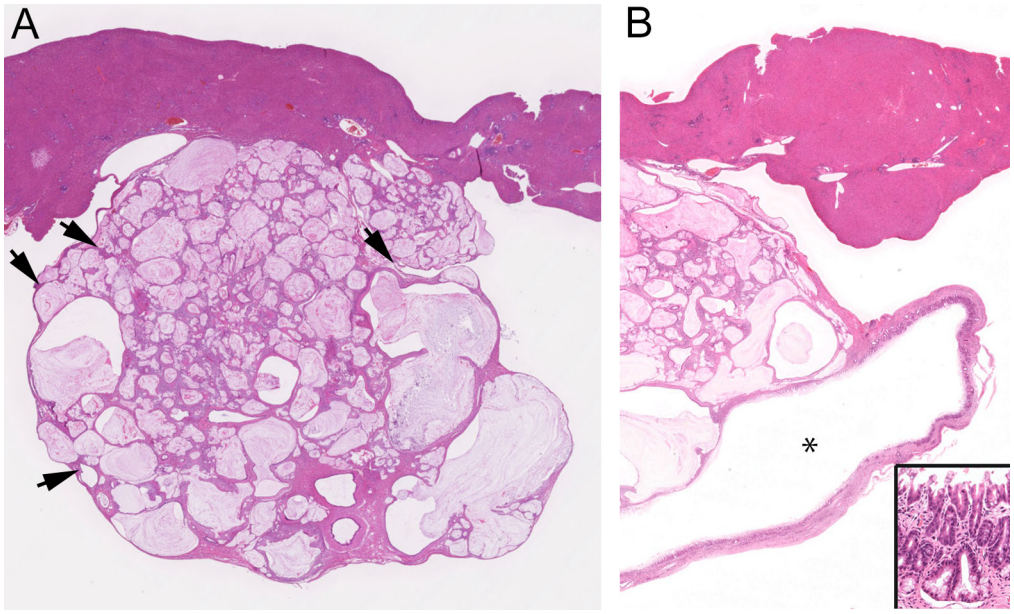

Fig. 2. **A**: Low-magnification image of mass showing expansive growth with no apparent compression of the liver. In the peripheral area of the mass, the hepatic parenchyma was randomly retained and retracted (arrows). The mass consisted of small to large dilated and/or tortuous ducts with abundant dense connective tissue. The dilated ducts were filled with mucus and cell debris. **B**: The peripheral area of the mass continued to the submucosa of a dilated common bile duct (asterisk). Inlet: The dilated common bile duct had a hyperplastic epithelium with intestinal metaplasia. HE stain.

The Ki-67 positivity index was estimated as the percentage of Ki-67-labeled nuclei/1,000 lining epithelial cells.

Histopathologically, the solitary mass showed expansive growth with no apparent compression of the liver (Fig. 2A). On the opposite side of the liver, the peripheral area of the mass continued to the submucosa of the dilated common bile duct, but with no apparent continuity to the mucosal epithelium (Fig. 2B). The dilated common bile duct had a hyperplastic epithelium with intestinal metaplasia (Fig. 2B). In the peripheral area of the mass, the hepatic parenchyma was randomly retained and retracted with small bile duct hyperplasia, but there was no apparent compression (Fig. 2A). The mass consisted of small to large dilated and/or tortuous ducts with sparse to abundant dense connective tissue and many inflammatory cells (Fig. 3). The dilated ducts were filled with AB-positive and PAS-positive mucus and cell debris (Fig. 4). The lining epithelium of the duct was single-layered and changed from cuboidal to columnar, flattened, and sometimes disappeared. The lining cells contained many goblet cells with AB-positive and PAS-positive mucus (Fig. 4). The surface of some lining cells showed a PAS-positive brush border. Nuclei were round to ovoid in shape, with small nucleoli, and located toward the basal side. Mitotic figures were often observed, and the Ki-67 positivity index of the lining cells was 10.0%. Immunohistochemically, the lining cells were positive for cytokeratin 7 (positivity rate: 80%), cytokeratin 19 (positivity rate: 80%), and OV-6 (positivity rate: 30%), which are bile duct markers (Fig. 5). Many inflammatory cells, including lymphocytes, plasma cells, and macrophages, were dispersed across the

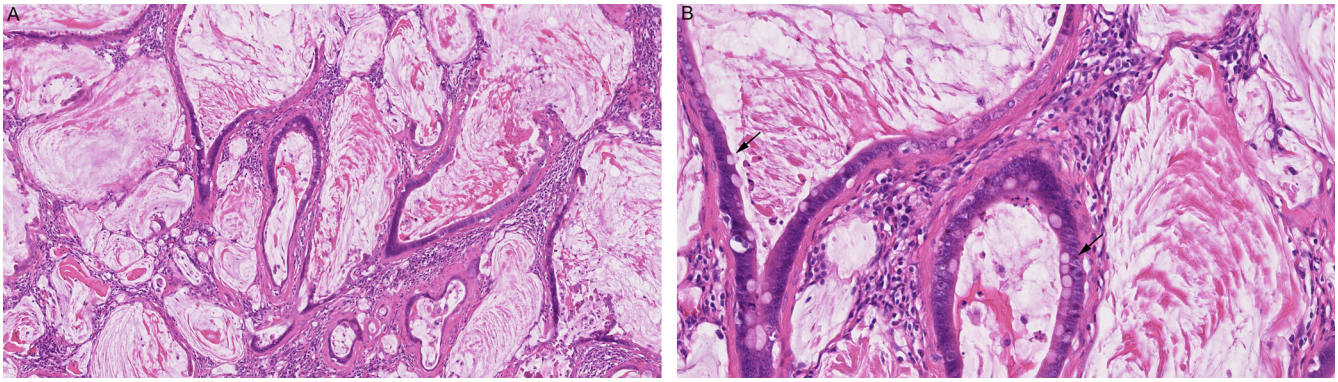

Fig. 3. **A**: High-magnification image of mass showing small to large dilated and/or tortuous ducts with abundant dense connective tissue and many inflammatory cells. **B**: Image showing the single-layer lining epithelium of the ducts. The lining epithelium contained many goblet cells (arrows) with mucus.

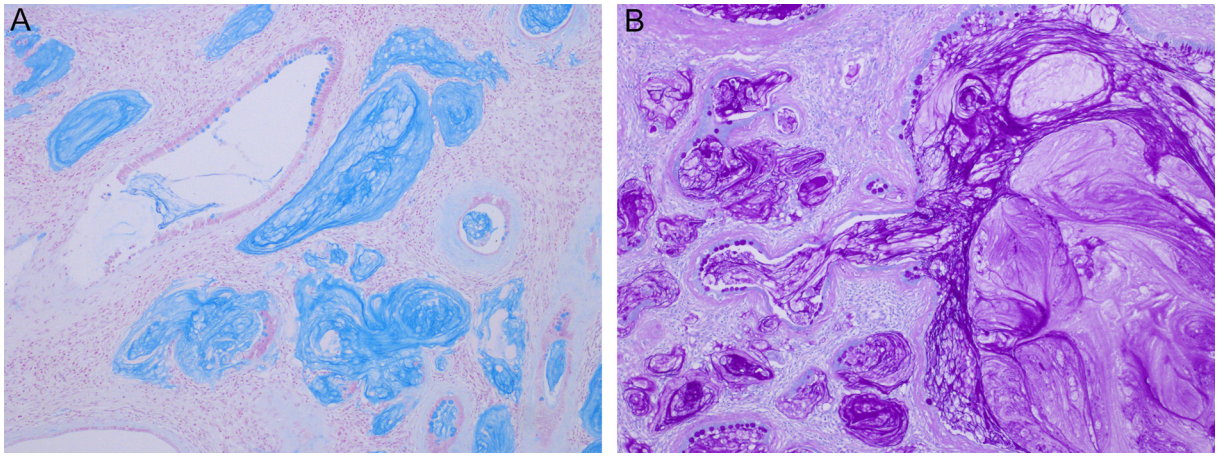

Fig. 4. Image showing mucus of the ducts and the goblet cells of the lining epithelium of dilated ducts with **A**: Alcian blue (AB)- and **B**: periodic acid–Schiff reaction (PAS)-positive mucus.

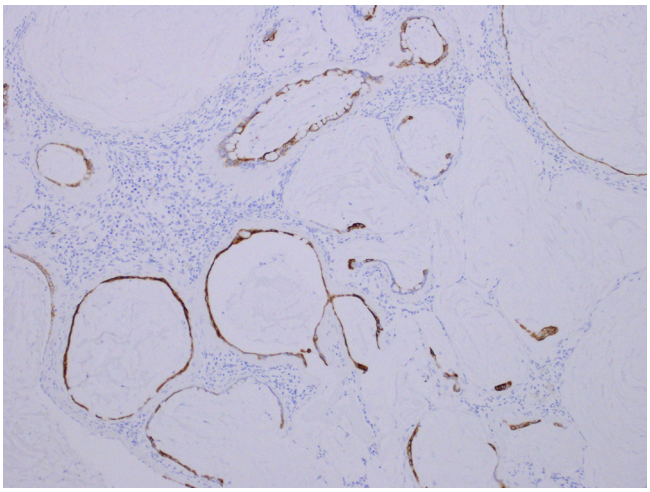

Fig. 5. Immunohistochemical image showing lining cells positive for cytokeratin 7.

dense fibrous stroma.

In the hepatic parenchyma adjacent to the mass, bile duct hyperplasia with/without fibrosis was observed with lymphoplasmacytic cell infiltration, but cholangiofibrosis of the hepatic parenchyma was not observed simultaneously.

Xenobiotic-induced cholangiofibrosis occurs in the hepatic parenchyma of multiple lobes in the liver[2–4]. It is characterized by retraction of the surrounding parenchyma, dilated and/or tortuous bile ducts with mucus, cuboidal to columnar lining epithelium with intestinal metaplasia, and abundant fibrous stroma with variable inflammatory cell infiltrates[1]. Cholangiofibrosis in LEC rats involves multiple lobes of the liver and has histological characteristics similar to those of xenobiotic-induced cholangiofibrosis[6]. The histopathological characteristics of our case were consistent with those of xenobiotic-induced cholangiofibrosis, and cholangiofibrosis in LEC rats[1–4, 6]. However, solitary mass formation and extracapsular proliferation differentiated our case from xenobiotic-induced cholangiofibrosis, and cholangiofibrosis observed in LEC rats. The spontaneous cholangio-

fibrosis reported by Chen was a solitary mass located at the hilus of the liver and had histopathological features similar to those of xenobiotic-induced cholangiofibrosis[5]. Our case resembled Chen's case of spontaneous cholangiofibrosis, except for continuity to a dilated common bile duct with intestinal metaplasia and hepatic parenchyma retained in the peripheral area. Recently, in the proceedings of the 2019 National Toxicology Program Satellite Symposium, spontaneous cholangiofibrosis in the liver and pancreas of untreated Hsd:Sprague Dawley (SD) rats was reported[10]. This case had histopathological descriptions similar to those of xenobiotic-induced cholangiofibrosis, but was different owing to the singular distribution and close proximity to a large bile duct. Hence, the hepatic and pancreatic lesions were termed "periductal cholangiofibrosis" to differentiate them from xenobiotic-induced cholangiofibrosis[10]. In our case, the cholangiofibrosis was characterized by its continuity to the large extrahepatic bile duct, similar to that observed in SD rats. Furthermore, the hyperplastic epithelium of the large bile duct showed intestinal metaplasia and cholangiofibrosis. These findings suggested that the primary site of the cholangiofibrosis in our case might be the extrahepatic bile duct. However, since no clear continuity from the extrahepatic bile duct epithelium could be confirmed, the primary site could not be identified. Based on the pathological characteristics, our case was diagnosed as spontaneous cholangiofibrosis adjacent to a dilated common bile duct with intestinal metaplasia.

The most important differential diagnosis was cholangiofibroma. The distinction between cholangiofibroma (neoplastic lesion) and cholangiofibrosis (non-neoplastic lesion) is difficult because of gradual transition[11, 12]. Bannasch stated that Chen's case of spontaneous cholangiofibrosis should be diagnosed as cholangiofibroma because of the expansive growth and protrusion of the liver surface[12, 13]. In contrast, Chen stated that the two terms need not be separated because a unique term for a cholangiofibroma is not available in INHAND and is dependent on the duration of the lesion[13]. Macroscopically, the mass formation in our case seemed to be neoplastic. However, since the lesion did not compress the liver parenchyma, and the mass randomly contained residual liver tissue, it was considered to have the characteristics of cholangiofibrosis, which is a non-neoplastic lesion. Other differentiations included cholangiocarcinoma and cholangioma. Carcinoma is differentiated by cell and structural atypia, whereas adenoma is characterized by no compression and frequent intestinal metaplasia.

The ducts in our case were positive for three types of bile duct markers, demonstrating that they originated from the bile duct. The characteristics of the three markers were as follows: cytokeratin 19 was present in all biliary structures[14], cytokeratin 7 was present in the large bile ducts, but absent in the small branch[14], and OV-6 was present in the bile ducts, including the Herring duct[4]. In our case, the positivity rate of cytokeratins 7 and 19 was high, whereas the positivity rate of OV-6 was low. Compared with Chen's case, ours was dominated by dilated bile ducts and a low positivity rate for OV-6, suggesting a long duration of the lesion[13].

We have reported cholangiofibrosis showing proliferation different from that of induced lesions; our case was diagnosed as spontaneous cholangiofibrosis adjacent to a dilated common bile duct with intestinal metaplasia.

Disclosure of Potential Conflicts of Interest: The authors declare that they have no competing interests.

References

1. Thoolen B, Maronpot RR, Harada T, Nyska A, Rousseaux C, Nolte T, Malarkey DE, Kaufmann W, Küttler K, Deschl U, Nakae D, Gregson R, Vinlove MP, Brix AE, Singh B, Belpoggi F, and Ward JM. Proliferative and nonproliferative lesions of the rat and mouse hepatobiliary system. Toxicol Pathol. **38**(Suppl): 5S–81S. 2010. [Medline] [CrossRef]
2. Wilson TM, Nelson PE, and Knepp CR. Hepatic neoplastic nodules, adenofibrosis, and cholangiocarcinomas in male Fisher 344 rats fed corn naturally contaminated with Fusarium moniliforme. Carcinogenesis. **6**: 1155–1160. 1985. [Medline] [CrossRef]
3. Hata M, Iida H, Yamanegi K, Yamada N, Ohyama H, Hirano H, Nakasho K, and Terada N. Phenotypic characteristics and proliferative activity of hyperplastic ductule cells in cholangiofibrosis induced by thioacetamide in rats. Exp Toxicol Pathol. **65**: 351–356. 2013. [Medline] [CrossRef]
4. Hickling KC, Hitchcock JM, Chipman JK, Hammond TG, and Evans JG. Induction and progression of cholangiofibrosis in rat liver injured by oral administration of furan. Toxicol Pathol. **38**: 213–229. 2010. [Medline] [CrossRef]
5. Chen T, Chen K, Qiu S, and Mann PC. Spontaneous cholangiofibrosis in a Wistar rat. Toxicol Pathol. **47**: 556–560. 2019. [Medline] [CrossRef]
6. Schilsky ML, Quintana N, Volenberg I, Kabishcher V, and Sternlieb I. Spontaneous cholangiofibrosis in Long-Evans Cinnamon rats: a rodent model for Wilson's disease. Lab Anim Sci. **48**: 156–161. 1998. [Medline]
7. Tsuji N, Ozaki K, Narama I, and Matsuura T. Inferior ectopic pupil and typical ocular coloboma in RCS rats. Comp Med. **61**: 378–384. 2011. [Medline]
8. LaVail MM, Sidman RL, and Gerhardt CO. Congenic strains of RCS rats with inherited retinal dystrophy. J Hered. **66**: 242–244. 1975. [Medline] [CrossRef]
9. Moroki T, Matsuo S, Hatakeyama H, Hayashi S, Matsumoto I, Suzuki S, Kotera T, Kumagai K, and Ozaki K. Databases for technical aspects of immunohistochemistry: 2021 update. J Toxicol Pathol. **34**: 161–180. 2021. [Medline] [CrossRef]
10. Elmore SA, Cesta MF, Crabbs TA, Janardhan KS, Krane GA, Mahapatra D, Quist EM, Rinke M, Schaaf GW, Travlos GS, Wang H, Willson CJ, and Wolf JC. Proceedings of the 2019 National Toxicology Program Satellite Symposium. Toxicol Pathol. **47**: 913–953. 2019. [Medline] [CrossRef]
11. Bannasch P, and Zerban H. Cholangiofibroma and cholangiocarcinoma, rat. In: ILSI Monographs on Pathology of Laboratory Animals, Digestive System, 2nd ed. TC Jones, JA Popp and U Mohr (eds). Springer, Berlin. 63–82. 1997.
12. Bannasch P. Letter to the editor regarding "Cholangiofi-

brosis and related cholangiocellular neoplasms in rodents". Toxicol Pathol. **47**: 896–898. 2019. [Medline] [CrossRef]
13. Chen T, and Mann PC. Response to letter to the editor regarding "Cholangiofibrosis and related cholangiocellular neoplasms in rodents". Toxicol Pathol. **47**: 899. 2019. [Medline] [CrossRef]
14. Paku S, Dezso K, Kopper L, and Nagy P. Immunohistochemical analysis of cytokeratin 7 expression in resting and proliferating biliary structures of rat liver. Hepatology. **42**: 863–870. 2005. [Medline] [CrossRef]